FORMATION OF NIOBIUM POWDER BY ELECTROLYSIS IN MOLTEN SALT

Isamu Ueda, Masahiko Baba, Tatsuya Kikuchi, and Ryosuke O. Suzuki

Faculty of Engineering, Hokkaido University

Kita-13 Jou, Nishi-8 chome, Kita-ku, Sapporo, 060-8628 Hokkaido, Japan

Abstract

Fine Nb_2O_5 powder was filled into a basket-type cathode and immersed in molten $CaCl_2$-0.5 mol% CaO at 1173 K. Nb_2O_5 immediately reacted with CaO in the molten $CaCl_2$ and formed calcium niobites that exhibited rod- or plate-like morphology. After the electrolysis of CaO with a graphite consumable anode, spherical particles of metallic niobium powder containing a residual oxygen concentration of 0.673 mass% O were obtained.

1. Introduction

Because of the high capacitance of Ta_2O_5, tantalum is a major material used in electrolytic capacitors. However, tantalum is scarce and expensive to produce. Niobium metal has many unique properties such as a high melting point, hydrogen absorption capacity, and superconductivity. In particular, the good electric properties of niobium metal make it a desirable alternative to tantalum for application in electrolytic capacitors. Many researchers have previously reported the possibility of using niobium as electrode material for electrolytic capacitors [1-6].

The electrodes of capacitors are currently fabricated by sintering metallic powder at high temperatures and by anodizing the surface of the sintered particles below 373 K to form an amorphous oxide film. The surface area of the electrode is determined by particle size and configuration, and it has a significant effect on the capacitance of the electrode. Because the sintering of particles decreases the surface area of the electrode, it is important to control the morphology of the metallic powder before sintering. For example, mixing fine spherical particles of tantalum with rod- or plate-like particles suppressed the decrease in the surface area of the electrode during sintering [7, 8]. It is thus expected that niobium powder having an analogous morphology will similarly minimize the decrease in the surface area of electrodes.

The industrial method for producing niobium powder consists of several processes [3, 9, 10]. Mined and concentrated ore is first reduced by aluminum metal (aluminothermic reduction). Because niobium metal produced by aluminothermic reduction often contains various impurities such as aluminum and oxygen, the crude

metal is purified using electron beam melting (EBM) under vacuum, and the molten pure niobium is solidified into ingots. The ingots are then pulverized using the costly method of hydrogenation and dehydrogenation (HDH).

For directly producing niobium powder from niobium oxide, many researchers have investigated alternative processes. Vahlas *et al.* [11] applied chemical vapor deposition (CVD) for preparing niobium powder. Fray *et al*. [12-18] used molten $CaCl_2$ to develop the "Fray, Farthing, and Chen" (FFC) Cambridge process. The reduction in FFC process is based on the oxygen ionization of cathodic metal oxides. However, after the metallic phase was obtained in a pellet, the niobium metallic particles sintered tightly in a long reduction time. Baba *et al*. [7, 8, 19] prepared Ta powder from fine Ta_2O_5 particles by Ca reduction in molten $CaCl_2$. The prepared Ta powder had a rod- or plate-like morphology, which was desirable for inhibiting particle coarsening in capacitor applications. Therefore, it is highly expected that Ca reduction of Nb_2O_5 can be used to prepare niobium powder having such morphology. It is noteworthy that this method would be unfavorable for application to large-scale production of niobium powder if the process consists of batch-type operations and if the reductant, Ca, is expensive. Because commercially available Ca contains high concentrations of various impurities, the impurities may be transferred into the niobium powder product.

Ono and Suzuki proposed the OS process [20,21] as a continuous method of using Ca to reduce stable oxides such as TiO_2 [20,22-26]. The same reduction mechanism that occurs during TiO_2 reduction with the OS method is expected to occur during Nb formation as follows. The solute, CaO, can dissolve in molten $CaCl_2$ up to 20 mol% [27] and form Ca^{2+} and O^{2-}.

$$CaO = Ca^{2+} + O^{2-} \text{ (dissolution of calcia)} \quad (1)$$

Ca^{2+} receives electrons from cathode and it is reduced to metallic Ca near the cathode. O^{2-} reacts with the carbon anode and forms a carbonic oxide (CO or CO_2).

$$Ca^{2+} + 2e^- = Ca \text{ (cathodic reaction)} \quad (2)$$

$$C + nO^{2-} = CO_n + 2ne^- \ (n=1 \text{ or } 2) \text{ (anodic reaction)} \quad (3)$$

The precipitated metallic Ca either directly reacts with niobium oxide near the cathode or dissolves into the $CaCl_2$ melt, and the strong reducing molten salt can form niobium from the oxide as follows:

$$Nb_2O_5 + 5\,Ca = 2\,Nb + 5\,CaO \text{ (reduction)} \quad (4)$$

CaO is the byproduct of Ca reduction, and it rapidly dissolves into the $CaCl_2$ melt and decomposes into ions, as shown in Eq. (1), which enables the continuous use of the OS process to recycle Ca without using any charge of the chemicals. Because the capacitor properties are sensitive to impurities, having a reductant with a neutral charge is a

significant advantage to prevent contamination.

In this study, we aim to use the OS process method for niobium oxides in order to produce metallic niobium powder that exhibit a rod- or plate-like morphology.

2. Experimental

The starting sample was Nb_2O_5 powder (99.9% pure), and its particle size was approximately 1 μm. The cathode was constructed as a basket-shaped container with a niobium disk and nickel net (300 mesh). The anode was a 10-mm-diameter graphite rod. Nb_2O_5 powder (2.0 g) was filled inside the cathodic container. Figure 1 shows the experimental apparatus. $CaCl_2$ (>95% pure; main impurity was water) and CaO (99.9% pure) were mixed in a composition of 99.5 mol% $CaCl_2$ and 0.5 mol% CaO. The mixture was placed into a MgO crucible (90-mm inner diameter; 200-mm deep), which was set in a stainless steel chamber. The apparatus was slowly heated at 873 K where $CaCl_2$ and CaO were dehydrated under vacuum for at least 20 ks. Argon gas saturated the apparatus, and the temperature was slowly increased to 1173 K. Two electrodes were inserted into molten salt at 1173 K, and a constant voltage of 2.8 V was applied. The electrolysis was terminated after a certain amount of electric charge was supplied, and the two electrodes were removed from the electrolyte before they were cooled. The samples in the cathodic container were placed into distilled water and were ultrasonically vibrated to remove the solidified salt. The sample powder was carefully separated from the container and was washed with a sequence of distilled water, acetic acid, distilled water, ethanol, and acetone. The samples were then dried and reserved under vacuum.

The phases in the samples were identified using X-ray diffraction (XRD) measurements with a Cu-Kα characteristic ray. The morphologies of samples were observed using scanning electron microscopy (SEM). The residual oxygen concentration in the samples was determined using the inert-gas-fusion infrared-absorption method with an oxygen/nitrogen analyzer LECO TC 600.

3. Results

3.1. Reaction without using electrolysis

Niobium oxide in the basket-shaped container was immersed into molten $CaCl_2$-0.5 mol% CaO without supplying any electric charge. After niobium oxide was immersed for either 1.8 or 3.6 ks, the container was raised to the upper part of the vessel and cooled. All the specimens were obtained as a lump with solidified $CaCl_2$. They were crushed into a fine powder, and the powder was washed with distilled water to remove

the solidified salt.

Figure 2 shows the XRD patterns for the samples that were immersed for either 1.8 or 3.6 ks. A large amount of calcium niobite ($CaNb_2O_6$) was formed with a small amount of Nb_2O_5 in these samples. Probably, $CaNb_2O_6$ was first produced in the molten salt by the reaction between the Nb_2O_5 powder and CaO. This is because $CaNb_2O_6$ is the most CaO-poor oxide in the quasi-binary Nb_2O_5-CaO system [28]. The Nb_2O_5 powder that was used consisted of fine particles (~1 μm in size), and the particles had a large surface area, so they easily reacted with the liquid CaO that was homogeneously dissolved in the molten salt as Ca^{2+} and O^{2-}. Therefore, $CaNb_2O_6$ could be quickly produced.

$$CaO(\text{ in molten } CaCl_2) + Nb_2O_5 = CaNb_2O_6 \quad (5)$$

Figure 3 shows the SEM images of the samples. Numerous particles exhibiting either rod- or plate-like morphology were formed. The particle size increased with increasing immersion time. The maximum length of the particles reached 200 μm, and several large twin crystals or large lumps composed of many primary particles are shown. Very few fine particles of the starting Nb_2O_5 powder are observed. These findings indicate that the reaction of Nb_2O_5 and CaO was very fast in the molten salt and that the formed $CaNb_2O_6$ has a characteristic morphology.

It is expected that $Ca_2Nb_2O_7$ may be produced by the reaction between $CaNb_2O_6$ and CaO after formation of $CaNb_2O_6$.

$$CaNb_2O_6 + CaO = Ca_2Nb_2O_7 \quad (6)$$

However, $Ca_2Nb_2O_7$ was not detected by XRD measurements. This is partially because the synthesized $CaNb_2O_6$ particles had a smaller surface area than the fine Nb_2O_5 powder.

3.2. Reduction by electrolysis of CaO

The theoretical charge (Q_0) is defined as the charge required in order to form the theoretical amount of Ca necessary to completely reduce the amount of Nb_2O_5 powder filled in the basket-shaped container. The supplied charge (Q) is calculated by integrating current with respect to time. Therefore, when $Q = Q_0$, the reactions given by Eqs. (2) and (4) should ideally complete to form metallic Nb without leaving any Nb_2O_5 powder residue. The ratio of Q/Q_0 is used as a normalized parameter to show the amount of supplied electric charge.

Figure 4 shows the XRD patterns for the obtained samples. The intensity of the diffraction peaks associated with Nb_2O_5 decreased with increasing Q/Q_0 and disappeared, even during the initial stage of electrolysis. NbO and calcium niobites

($Ca_nNb_2O_{5+n}$, where n = 1 or 2) were commonly detected in the samples whose Q/Q_0 = 49 and 110%. It is noteworthy that NbO is an intermediate phase between Nb_2O_5 and Nb in the binary Nb-O system and that $CaNb_2O_6$ and $Ca_2Nb_2O_7$ could coexist.

In the diffraction measurements for the samples whose $Q/Q_0 \geq 192\%$, the XRD peaks associated with the lower oxides, such as NbO, and the calcium niobites had completely disappeared, and only peaks associated with pure Nb were identified. The shift of XRD diffraction peaks of Nb corresponds to the shrinkage of Nb lattice due to oxygen loss from the Nb-O solid solution.

Figure 5 shows the residual oxygen concentration in the samples after electrolysis. The residual oxygen concentration decreased with increasing supplied charge, Q/Q_0. It is also clear from the analysis of the residual oxygen concentration that niobium oxides were not completely reduced at Q/Q_0 = 100% because the precipitated calcium diffused from the cathode into the bulk and because the lower oxide and calcium niobite required higher calcium activity. The low residual oxygen concentration of 0.673 mass% was achieved in the sample electrolyzed at Q/Q_0 = 500%.

Figure 6 shows the SEM images of the reduced samples. Fine Nb_2O_5 powder became coarser and more spherical as Q/Q_0 increased. The rod- or plate-like morphology was found in the samples electrolytically reduced at Q/Q_0 = 49 and 110%. The size of the largest rod- or plate-like particle was about 100 μm. From the XRD data, as shown in Fig. 4, these particles correspond to the calcium niobites. The morphology of the samples became spherical at $Q/Q_0 > 150\%$, and the spherical particles (3–5 μm in diameter) were dominant in the sample electrolytically reduced at Q/Q_0 = 500%. The change in morphology reflects the metallization of calcium niobites. It is noted that the crystalline lattices of the complex oxides $CaNb_2O_6$ and $Ca_2Nb_2O_7$ are orthorhombic and cubic, respectively. It is certain that the anisotropic oxide particles were reduced to the spherical metal powder.

4. Discussion

4.1. Morphology and reduction rate

Most of the Nb_2O_5 particles quickly reacted with CaO in molten $CaCl_2$ at a very early stage, and they became coarse $CaNb_2O_6$ particles that exhibited rod- or plate-like morphology. $CaNb_2O_6$ is thermodynamically stabler than Nb_2O_5 [29] if CaO coexists, and the formation of coarse calcium niobite particles decreases the surface area of the oxide, which should decrease the rate of Ca reduction. These are the reasons that the rate of reduction was decreased and that a significant electrolytic time was necessary in order to prepare pure niobium.

4.2. Formation of $Ca_2Nb_2O_7$

$Ca_2Nb_2O_7$ coexisted with $CaNb_2O_6$ during electrolytic reduction, as mentioned in section 3.2. However, $Ca_2Nb_2O_7$ was not formed during the experiment performed without using electrolysis, as mentioned in section 3.1. It is expected that CaO is locally abundant near the $CaNb_2O_6$ crystals because the decrease in the valence of Nb from +5 (in $CaNb_2O_6$) to +2 (in NbO) generates CaO, as expressed in Eq. (7).

$$CaNb_2O_6 + 3\,Ca = 2\,NbO + 4\,CaO \quad (7)$$

The produced CaO quickly dissolves into the molten salt, and the activity of CaO near calcium niobite becomes higher than that of CaO in other areas. $Ca_2Nb_2O_7$ thus forms more easily, as per Eq. (6). That is the reason that the XRD peaks were identified as the peaks associated with $Ca_2Nb_2O_7$.

Equations (6) and (7) taken together indicate the possible existence of a three-phase equilibrium among $CaNb_2O_6$, NbO, and $Ca_2Nb_2O_7$ in the ternary Nb-Ca-O system. Taken together with the isothermal section of the binary Nb-O [29] and quasi-binary Nb_2O_5-CaO phase diagrams [28], the isothermal section of the ternary Nb-Ca-O phase diagram can be expected, as shown in Fig. 7. If lower oxides do not exist in the quasi-ternary Nb_2O_5-CaO-Ca region, all the components on the Nb-O and Nb_2O_5-CaO lines should be connected based on the thermodynamics of the materials. Supposing that $CaNb_2O_6$ equilibrates with $Ca_2Nb_2O_7$, we can draw several tie lines in the isothermal sections, as shown in Fig. 7.

The line between $Ca_2Nb_2O_7$ and Nb shown in Fig. 7 is thus one of the speculated lines, indicating the reduction path for the $Ca_2Nb_2O_7$ phase.

$$Ca_2Nb_2O_7 + 3Ca = 2NbO + 5CaO \quad (8)$$

$$Ca_2Nb_2O_7 + 5Ca = 2Nb + 7CaO \quad (9)$$

The starting Nb_2O_5 powder reacts with CaO to form $CaNb_2O_6$, which is then reduced to Nb via NbO when the reducing condition is strong. When the reducing condition is mild, however, $CaNb_2O_6$ decomposes to supply CaO in order to form $Ca_2Nb_2O_7$. Part of this CaO-rich phase can be reduced via NbO to Nb.

$$NbO + Ca = Nb + CaO \quad (10)$$

However, another part of $Ca_2Nb_2O_7$ can be directly reduced to Nb, not via NbO.

The ternary Nb-Ca-O phase diagram shown in Fig. 7 may be revised in future because it is derived based on the XRD data obtained during electrolysis and may therefore exclude the possible existence of other phase equilibria; for example, a new ternary compound or lower complex oxide. Still, the assistance of the ternary Nb-Ca-O phase diagram promotes phase identification during reduction and phase analysis of the

possible paths for the reduction of the NbO to metallic Nb. It is clear that metallic Nb can be formed at least through several phases and several reduction paths. This reduction path analysis suggests the reason for the wide variety of morphologies obtained for the metallic Nb particles.

4.3. Pulverization of Nb

The obtained niobium powder that has the lower oxygen concentration exhibits the common coarse-particle morphology. Although it is difficult to prepare metallic niobium powder that only exhibits rod- or plate-like morphology, Ca reduction of Ta_2O_5 could produce such structures [7, 8]. The reason is as follows: Large and long particles of calcium niobite were attacked by Ca metal, and they shrank locally. The densities of $CaNb_2O_6$ and Nb metal are 4.75 and 8.56 g/cm^3, respectively [30, 31]. As illustrated in Fig. 8, coarse particles of $CaNb_2O_6$ are broken into smaller ones because of the stress of volume constriction. The reduced Nb particles are thus finer than either $CaNb_2O_6$ or $Ca_2Nb_2O_7$ particles but are much coarser than the original fine Nb_2O_5 powder.

4.4. Carbon contamination

CO and CO_2 gases are produced near the graphite anode during electrolysis, as shown in Eq. (2). Although these gases should be expelled to the outside of the vessel, they can partially react with Ca near the cathode and sometimes form CaO and carbon [32]. As this CaO also dissolves into the melt, the origin of the oxygen cannot be distinguished as coming from either the CaO or the starting oxide. Because carbon does not dissolve, carbon powder would be expected to form on the salt surface or in the molten salt. In fact, a black powder was found at the surface of the solidified salt. This induces carbon contamination, and niobium carbide (NbC) that appeared during the later stage of reduction (at the larger Q/Q_0) is evidence of this parasite reaction. Carbon contamination seriously affects the characteristics of niobium, especially when niobium is used in capacitor applications. Shorter electrolysis times are therefore desirable to prevent carbonization of the produced niobium.

5. Conclusions

Calcium niobites that exhibited either rod- or plate-morphology were formed by immersing Nb_2O_5 into molten $CaCl_2$-CaO without using any electrolytic charge. During the initial stage of electrolytic reduction, calcium niobite particles that exhibited either rod- or plate-like morphology were formed. Calcium niobites gradually became metallic niobium powder during reduction. The Nb-metal particles electrolytically reduced at

Q/Q_0 = 500% were small and spherical and had a residual oxygen concentration of 0.673 mass% O. This work suggests possibilities of applying calciothermic reduction of Nb_2O_5 operated using the electrolysis of CaO in molten $CaCl_2$ to prepare metallic niobium powder.

References

[1] T. H. Okabe: Mater. Jpn. (Bull. Jpn. Inst. Met.) 43 (2004) 34.

[2] S. Luidold, H. Antrekowitsch, R. Ressel: Int. J. Refractory Met. Hard Mat. 25(5) (2007) 423.

[3] B. Yuan, T. H. Okabe: J. Alloys Comp. 454 (2008) 185.

[4] H. Störmer, A. Weber, V. Fischer, E. Ivers-Tiffée, D. Gerthsen: J. Eur. Ceram. Soc. 29(9) (2009) 1743.

[5] W. A. Serjak, L. Shekhter, T. B. Tripp, L. L. Lanin, K. Reichert, O. Thomas: Proc. 20th Passive Components Symposium (CARTS USA) (2000), pp. 82.

[6] P. Kathirgamanathan, S. Ravichandran: Synthetic Metals 74 (1995) 165.

[7] R. O. Suzuki, M. Baba, Y. Ono, K. Yamamoto: J. Alloys Comp. 389 (2005) 310.

[8] M. Baba, R. O. Suzuki: J. Alloys Comp. 392 (2005) 225.

[9] I. G. Sharna, S. P. Chakraborty, D. K. Bose: J. Alloys Comp. 236 (1996) 216.

[10] S. B. Gabriel, G. Silva, K. C. G. Cabdioto, I. D. Santos, P. A. Suzuki, C. A. Nunes: Int. J. Refractory Met. Hard Mat. 29(1) (2011) 134.

[11] C. Vahlas, B. Caussat, P. Serp, G. N. Angelopoulos: Mater. Sci. Eng. R Reports 53(1) (2006) 1.

[12] D. J. Fray, T. W. Farthing, Z. Chen: International Patent, WO99/64638 (1999).

[13] A. M. Abdelkader, D. J. Fray: Electrochim. Acta 55(8) (2010) 2924.

[14] M. Ma, D. Wang, W. G. Wang, X. H. Hu, X. B. Jin, G. Z. Chen: J. Alloys Comp. 420(1-2) (2006) 37.

[15] A. M. Abdelkader, D. J. Fray: J. Eur. Ceram. Soc. 32(16) (2012) 4481.

[16] A. M. Abdelkader, D. J. Fray: Electrochim. Acta 64 (2012) 10.

[17] E. Gordo1, G. Z. Chen, D. J. Fray: Electrochim. Acta 49 (2004) 2195.

[18] X. Y. Yan, D. J. Fray: Metall. Mater. Trans. B 33B(5) (2002) 685.

[19] M. Baba, Y. Ono, R. O. Suzuki: J. Phys. Chem. Solid 66(2-4) (2005) 466.

[20] R. O. Suzuki, K. Teranuma, K. Ono: Metal. Mater. Trans. B 34(3) (2003) 287.

[21] R. O. Suzuki, S. Inoue: Metal. Mater. Trans. B 34B (2003) 277.

[22] K. Ono, R. O. Suzuki: JOM Mem, J. Min. Met. Mater. Soc. 54(2) (2002) 59.

[23] R. O. Suzuki, K. Tatemoto, H. Kitagawa: J. Alloys Comp. 385 (2004) 173.

[24] R. O. Suzuki: J. Phys. Chem. Solid 66 (2005) 461.

[25] R. O. Suzuki, S. Fukui: Mater. Trans. 45 (2004) 1665.
[26] R. F. Descaller-A., N. Kobayashi, T. Kikuchi, R. O. Suzuki: Electrochim. Acta, 56 (2011) 8422.
[27] G. S. Perry, L. G. Macdonald: J. Nucl. Mater. 130 (1985) 234.
[28] M. Ibrahim, N. F. H. Bright, J. F. Rowland: J. Am. Ceram. Soc. 45(7) (1962) 329.
[29] R. P. Elliott: Trans. Am. Soc. Met. 52 (1960) 990.
[30] H. Trumpour: Am. Mineral 44 (1959) 1.
[31] M. Nadler, C. Kempter: Anal Chem., 31 (1956) 1922.
[32] K. Otake, H. Kinoshita, T. Kikuchi, R. O. Suzuki: J. Phys. Conf. Ser., 379 (1) (2012) 012038.

Figure captions

Fig. 1. Experimental setup used in this work.
Fig. 2. XRD patterns for samples immersed for 1.8 or 3.6 ks. Electrolysis was not applied.
Fig. 3. SEM images of samples immersed for (a) 1.8 or (b) 3.6 ks.
Fig. 4. XRD patterns for samples obtained after electrolysis.
Fig. 5. Relation between supplied charge and residual oxygen concentration.
Fig. 6. SEM images of samples obtained after electrolysis.
Fig. 7. Isothermal phase diagram for Nb-Ca-O ternary system.
Fig. 8. Illustration of change in morphology due to reduction.

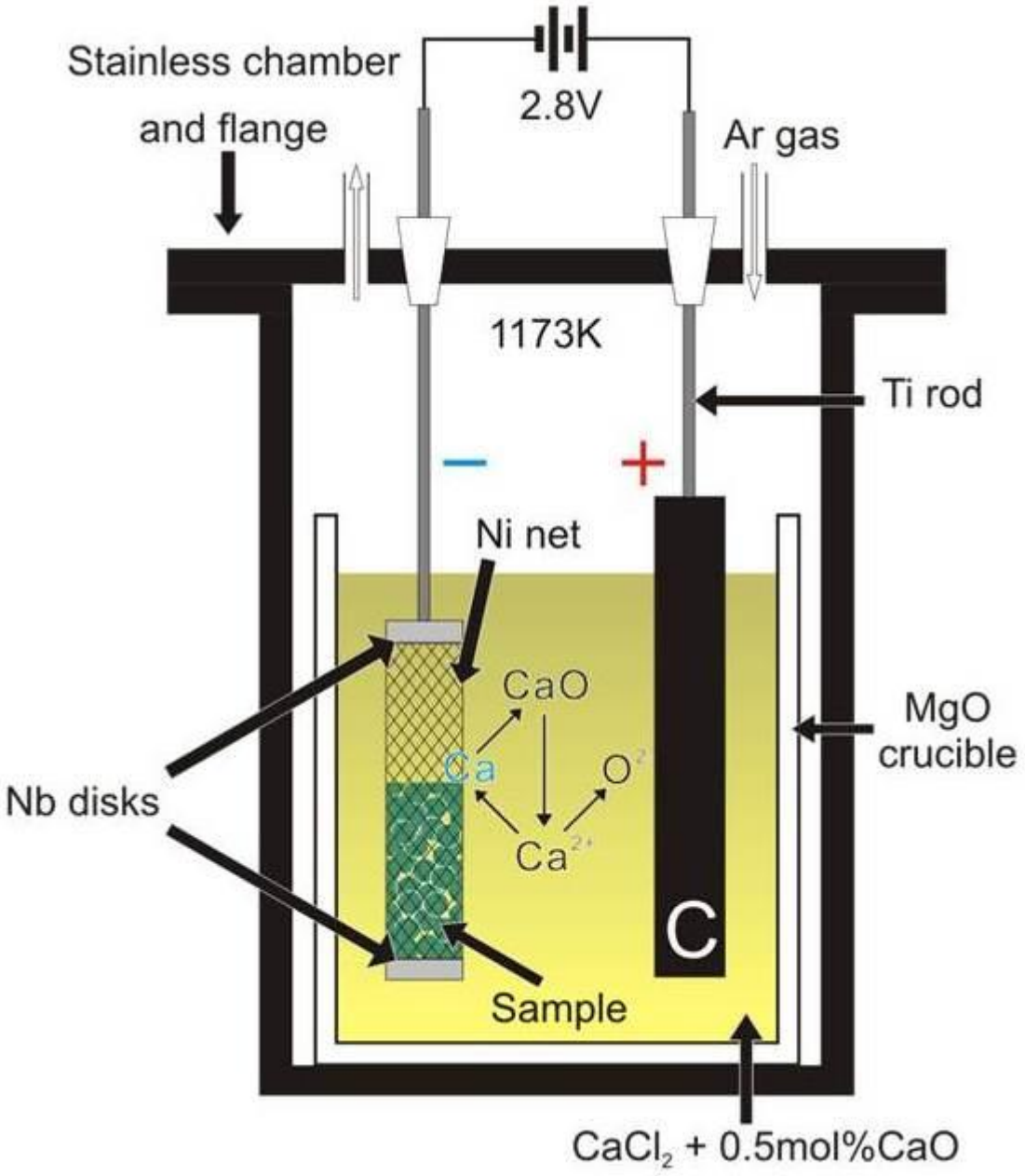

Fig. 1. Experimental setup used in this work.

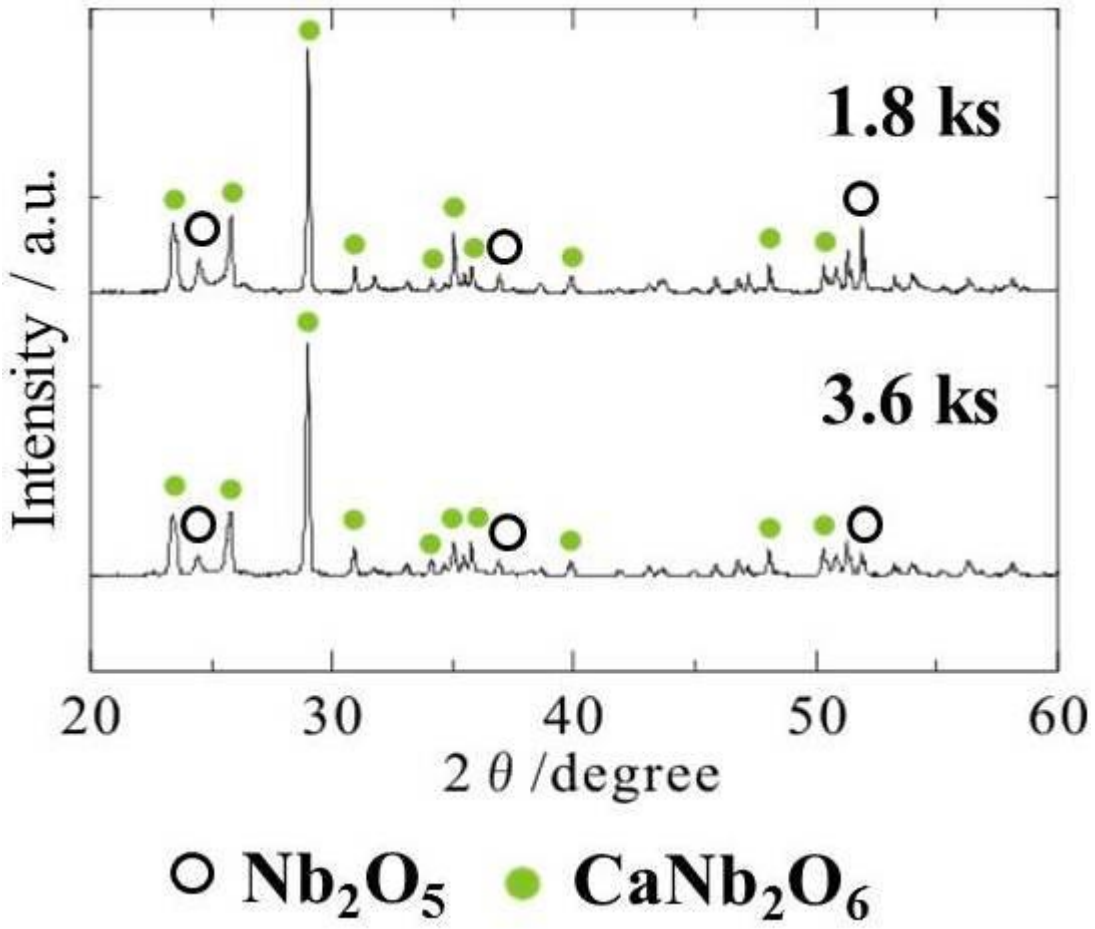

Fig. 2. XRD patterns for samples immersed for 1.8 or 3.6 ks. Electrolysis was not applied.

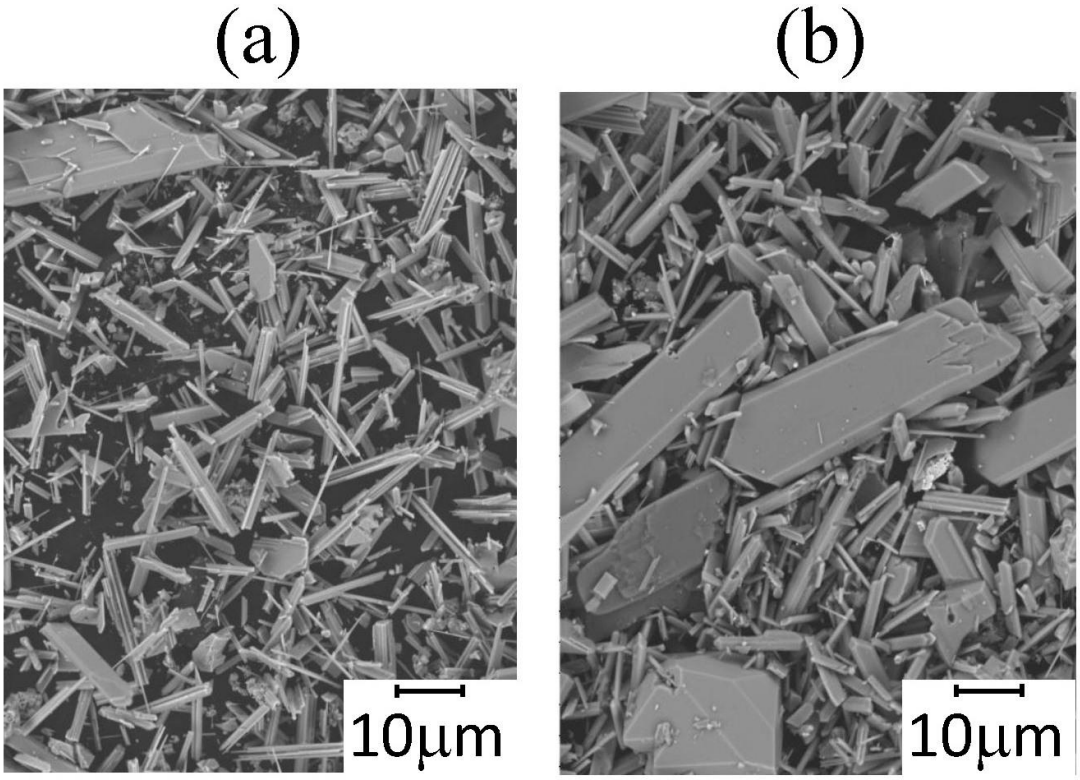

Fig. 3. SEM images of samples immersed for (a) 1.8 or (b) 3.6 ks.

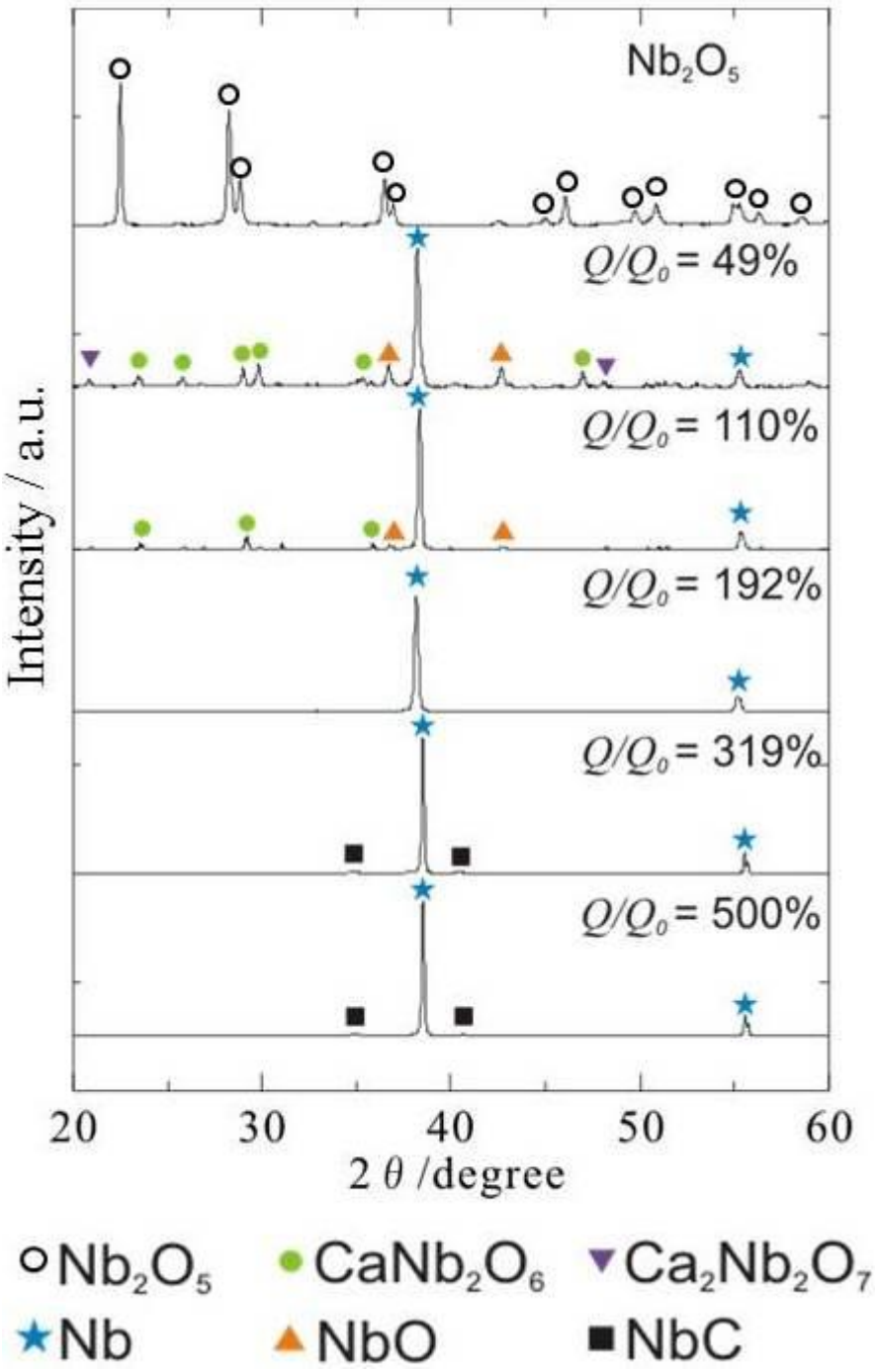

Fig. 4. XRD patterns for samples obtained after electrolysis.

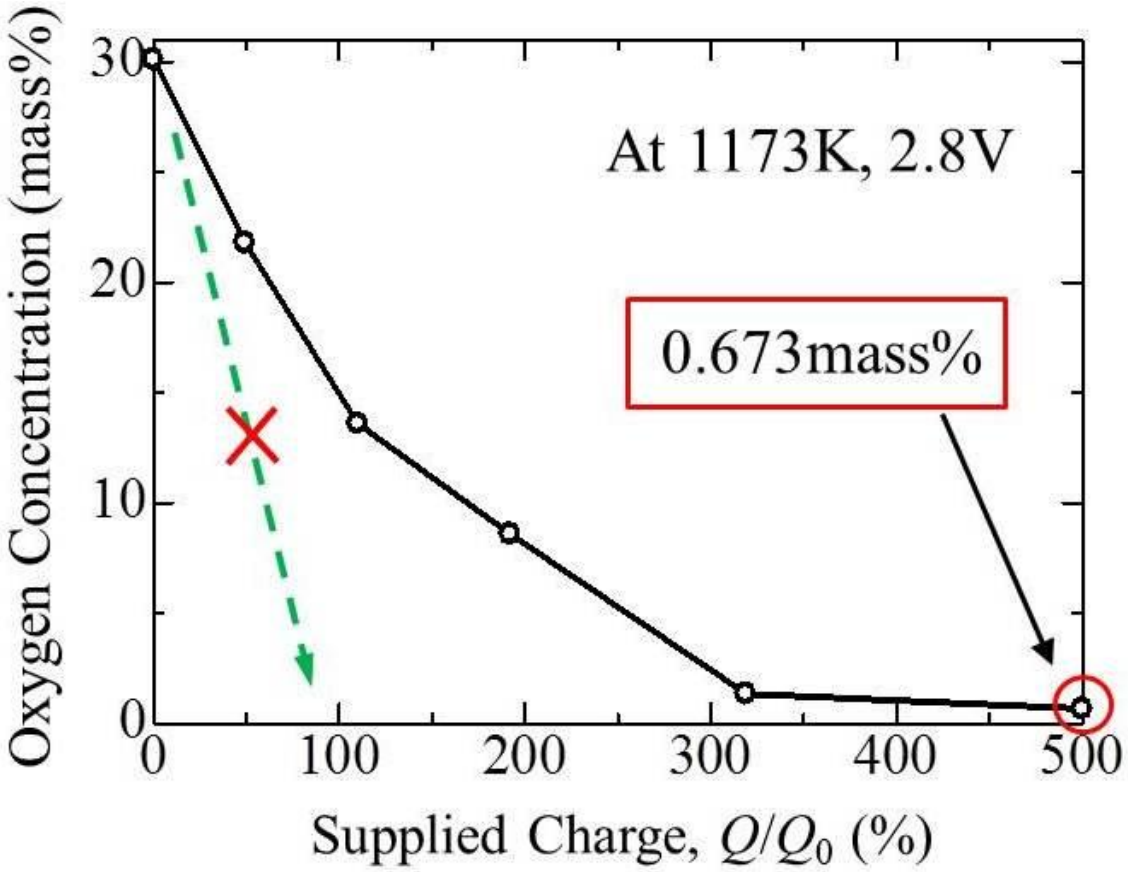

Fig. 5. Relation between supplied charge and residual oxygen concentration.

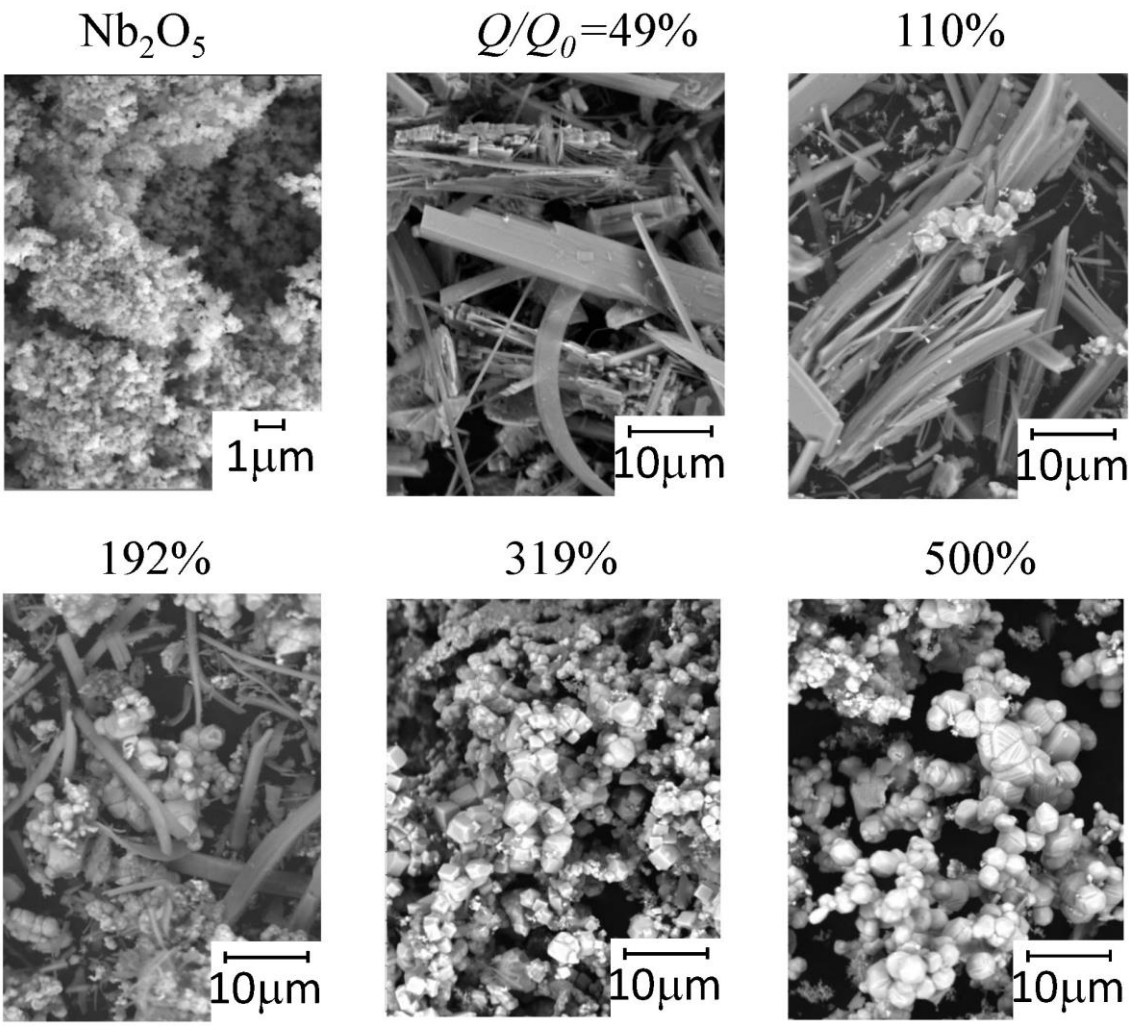

Fig. 6. SEM images of samples obtained after electrolysis..

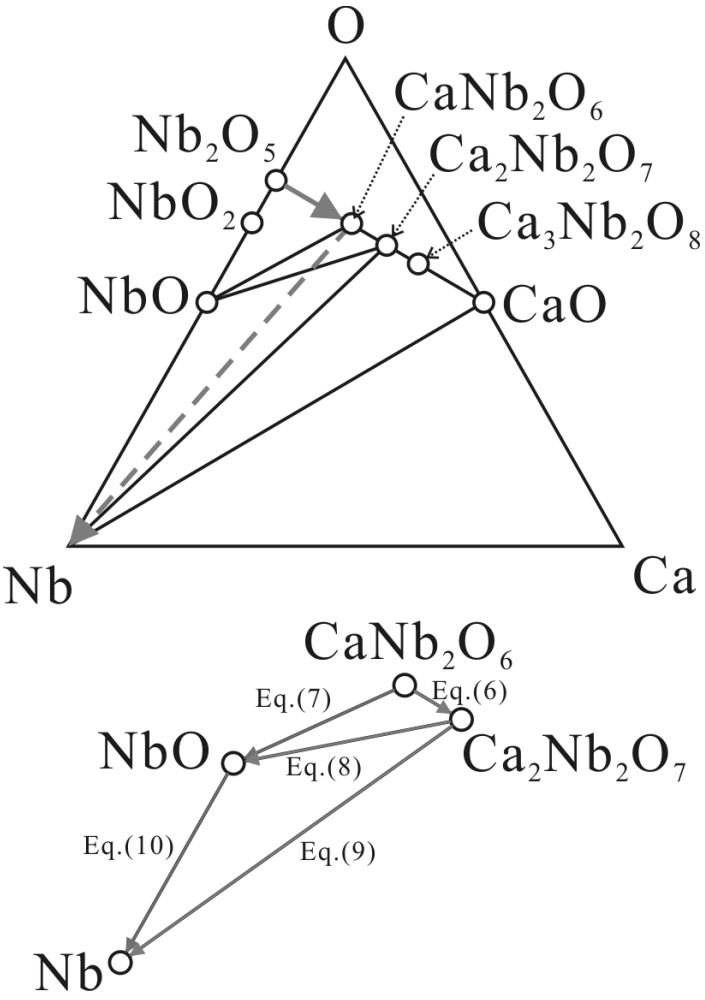

Fig. 7. Isothermal phase diagram for Nb-Ca-O ternary system.

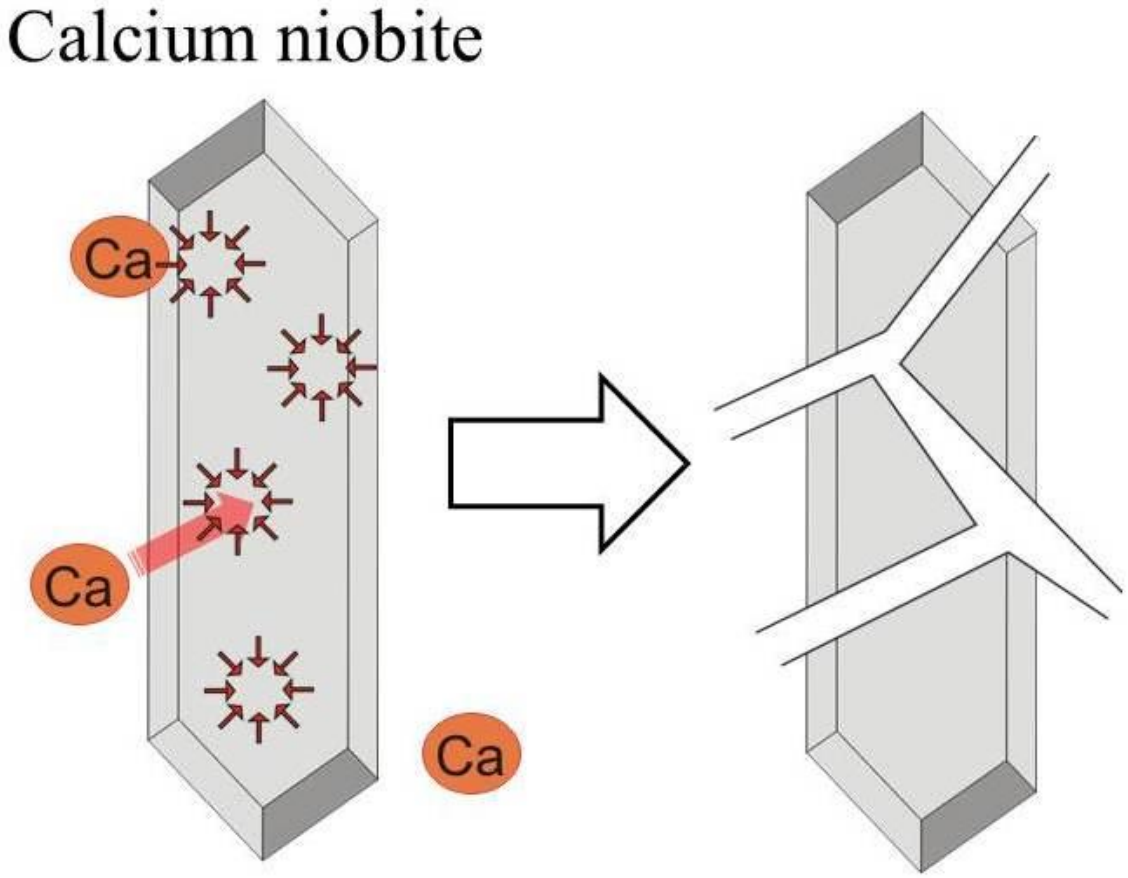

Fig. 8. Illustration of change in morphology due to reduction.